UCRL-JC-125383
PREPRINT

Towards Predicting the Laser Damage Threshold of Large-area Optics

J. Hue
F. Genin
S. Maricle
M. Kozlowski

This paper was prepared for submittal to the
Symposium on Optical Materials for High Power Lasers '96
Boulder, CO
October 7-8, 1996

October 1, 1996

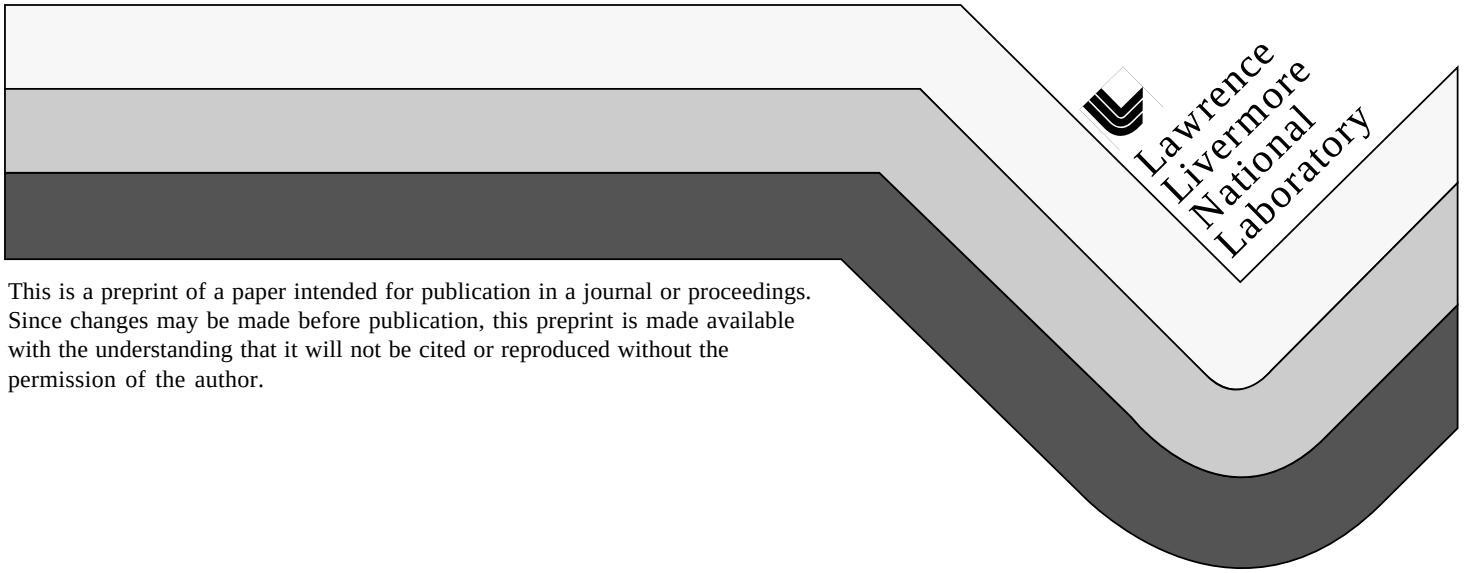

Towards predicting the laser damage threshold of large-area optics

Jean Hue
LETI - CEA - DOPT- Couches Minces pour l'Optique (CMO), CENG,
17, Avenue des Martyrs, 38054 Grenoble, Cedex 09, FRANCE.
((33)-76-88-99-31, Fax : (33)-76-88-50-46

François Y. Génin, Stephen M. Maricle, Mark R. Kozlowski
Lawrence Livermore National Laboratory,
Livermore, California 94550, USA.

ABSTRACT

As the size of optics has increased, so has the difficulty in effectively measuring and defining their laser damage threshold. This is exemplified in the case of optical coatings being developed for the National Ignition Facility (NIF) in the USA and the Laser MegaJoules (LMJ) in France. Measuring the threshold on small witness samples ($\leq cm^2$) rather than on the full aperture optic ($\approx m^2$) presents obvious advantages. In this article, the threshold of large-area components is being addressed in two general ways that both use experimental mapping data.

First, a model based on the fruitful concept of the R-on-1 threshold distribution is shown to predict the threshold of a large optic with a high degree of confidence. At the same time, it is determined that the average R-on-1 threshold provides a reliable and accurate value to evaluate the coating improvements. To acquire the essential data, an automated damage test bench has been developed by the laboratory of "Couches Minces pour l'Optique" (CMO) at the "Commissariat à l'Energie Atomique" (CEA).

Secondly, the damage threshold has to be defined according to the final use of the component. To address this issue, the Lawrence Livermore National Laboratory (LLNL) has defined a functional damage threshold to set limits on the maximum damage size. An empirical power law dependence of average damage size on peak fluence was found. This relation can be used to predict the damage behavior of large-aperture optics exhibiting the same damage morphology.

Keywords : threshold distribution, statistical information, functional threshold, large-area optics, damage size, damage morphology, threshold mapping, laser-induced damage.

1. INTRODUCTION

Today, for the damage threshold of large-area optics ($\approx m^2$) of high fluence lasers such NOVA or PHEBUS, engineers use the following rule of thumb : the laser damage threshold of small witnesses ($\leq cm^2$) needs to be double the required fluence in order for the large-area optics to withstand the required fluence. The next generation of lasers (NIF and LMJ) contain numerous optics. These optics will have to withstand a fluence larger than the optics of the previous generation with a higher degree of reliability. Today, the tests done on large optics show the inefficiency of the rule of thumb for numerous optics. A method of measurement and a defined threshold needs to be found to address the problem with a high degree of reliability for numerous large optics. In this article, two different methods to predict the threshold of large-area optics from studying a selected area of a witness sample are proposed.

An automated damage testing station (ADT)[1] provided the R-on-1 data which are analyzed in the first section of this paper. From these experiments, two important concepts appear : first the R-on-1 average threshold and secondly, the threshold distribution. The R-on-1 average threshold will allow a comparison without a doubt of the resistance to damage of various components. The threshold distribution with the help of a model will allow a prediction of the maximum fluence that will not damage a large-aperture optic.

In the second section, another characterization method is proposed. It is based on 1-on-1 tests. These tests allow a determination of the correlation between the damage size and the peak fluence. Frequently, only the damage threshold is published and sometimes the damage morphology is reported. Some papers have studied the threshold of a variety of damage morphologies[2]. It is unusual to shoot during the laser tests beyond the threshold to obtain more information[3]. At LLNL, tests are in progress to determine the "functional damage" threshold of optics based on some allowable degree of damage.[4,5,6]

2. LARGE-AREA THRESHOLD : R-ON-1 THRESHOLD DISTRIBUTION

Many articles provide a method which yields a threshold independent of the spot size.[7,8,9] Based on these studies, a draft international standard[10] was developed. Other papers suggest improvements of the previous method to accelerate measurements and improve the accuracy[11,12]. Several authors[13] have already used the threshold distribution to study the effect of sample parameters (e.g. roughness, thickness of undercoat,etc...) on the damage threshold. However, they have not addressed the issue by taking into account the threshold distribution of the number of sites tested. At LLNL, a damage test system has been designed to laser condition large optics[14]. On going tests are conducted to determine how the threshold of a large optic differs from that of a witness sample.

The experimental set-up and the data used are briefly summarized in the first part. Then, the effect of the spot size and the effect of the number of sites are discussed. This discussion leads to the concept of the average R-on-1 threshold. Next, the threshold distribution is studied. With the threshold distribution, a prediction of the damage threshold for a large-area becomes possible. Finally, the general method used to reach this crucial result is summarized.

2.1 Set-up and experimental data

The set-up and the experimental data have been already presented elsewhere[1,15]. Only the details needed to understand this study are reminded. The values chosen to illustrate the method were measured on a high reflector tested at 355 nm, 3 ns with a R-on-1 procedure on 441 sites (Fig.1). The beam was close to a Gaussian beam with an area at $1/e^2$ of about 1 mm^2. In this paper, to simplify the discussion, the beam size is assumed to be a top-hat with an area of 1 mm^2. In the following, this unit area will be called "s" and the total number of sites "N" (N=441).

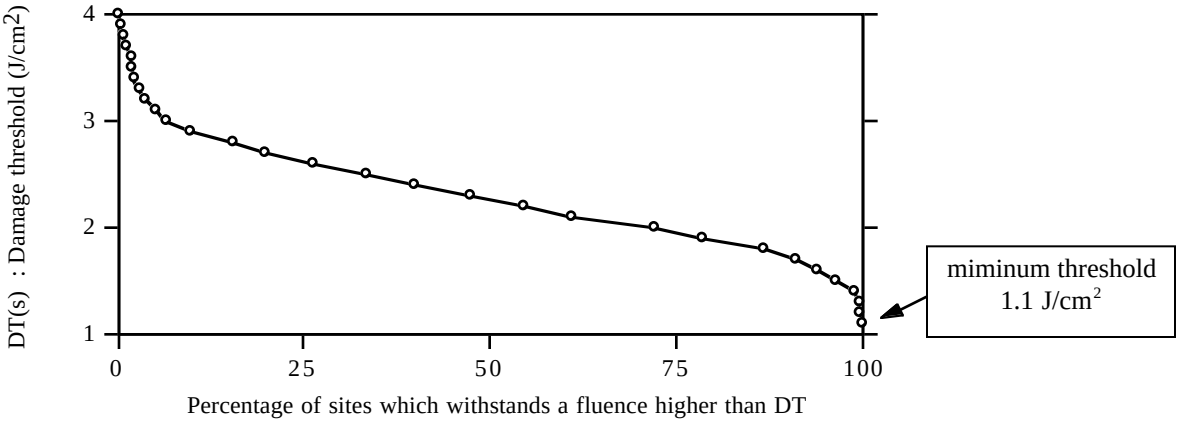

Beam size : s

Experimental data : R-on-1 laser damage thresholds of N sites (Fig. extracted from ref. 15)

Figure 1

2.2 Thought experiments from experimental data

With the numerous data plotted in Figure 1, it becomes possible to test again, by the thought, exactly the same area. The tests can be done with different beam sizes as well as different number of size to evaluate the effect of this two parameters on the damage threshold.

2.2.1 Spot size effect

Figure 1 is obtained with a spot size of area s, for a total area equal to Ns. Let us imagine a sample of Ns area have been tested. By thought, it is possible to test exactly the same area with different spot sizes. For instance, the threshold of the first site tested with a 3s area is provided by keeping the lower threshold value of the first 3 sites tested with a beam size s and so on for the other values tested with a 3s area. In this way, for a 3s beam size, N/3 threshold values will be provided. These results obtained following this method are summarized in Figure 2.

For the various sizes, it is obvious that the only constant is the lower threshold value : 1.1 J/cm^2 (Fig. 2a). The method proposed by Foltyn[7] allows to obtain the same threshold with different spot sizes. However, an obvious condition has to be added : the threshold is exactly the same if exactly the same area is tested.

The threshold is driven by the weakest point of the component. Therefore, the thresholds of large components of 50 cm x 50 cm (typical size for the LMJ and NIF) are difficult to predict. From this analysis, the first conclusion for a similar but "larger" optic is : the threshold will not exceed 1.1 J/cm^2, the lowest threshold measured on the small part (see Figs.1 and 2). It is the upper limit that a large aperture optic will not exceed.

Other conclusions are:

- The average and the maximum threshold fluences decrease when the beam size increases. Indeed, a beam size acts as a low-pass filter (see Fig.2a). Consequently, the threshold of a component decreases when its tested area increases.
- The standard deviation and the ratio between the standard deviation and the average threshold value decrease until a beam size equal to 21 s (see Fig.2b). For a beam size larger than 21s, the standard deviation increases, probably because the number of data points decreases. Indeed, the total area is constant : Ns = (number of sites) x (beam size) = (Ns/Y) x (Ys). Therefore when the beam size increases the number of sites decreases. For instance, for a 147s beam size, we have only 3 experimental values while for a 1s beam size, we have 441 data.

number of sites (Ns/Y)	beam size (unity "s") (Ys)	same area and same tested surface Ns= (Ns/Y) x (Ys)
1	441 s	1 x 441s = 441s
3	147 s	3 x 147s = 441s
7	63 s	7 x 63 s = 441s
21	21 s	21 x 21s = 441s
63	7 s	63 x 7s = 441s
147	3 s	147 x 3s = 441s
441	1 s	441 x 1s = 441s

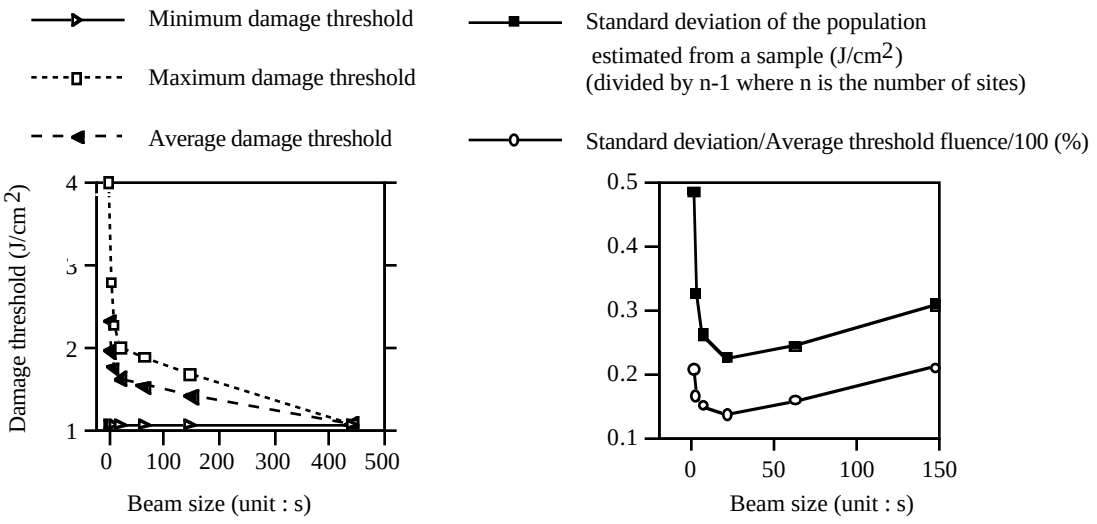

Figure 2a **Figure 2b**

Statistical parameters versus beam size : thought experiments from real data of the same area (N s)

Figure 2

2.2.2 The average R-on-1 threshold (the effect of the number of sites)

Figure 3 shows the statistical parameters respectively for a spot size s and 7s as a function of the number of sites. The average R-on-1 threshold and the standard deviation become almost constant as soon as

the number of sites becomes larger than 7. The R-on-1 average depends on the spot size. It is not the threshold of the component for final use. But, it is interesting to use the R-on-1 average threshold :
- to study the effect of various parameters (coating preparation, substrate cleaning[19], pulse duration, etc...),
- and to compare different test benches (with the same spot size).

The study of the distribution of the R-on-1 average threshold would demonstrate that the R-on-1 average threshold leads to a constant whatever the shape of the distribution (central limit theorem[16]). Indeed, this result is easy to explain : the larger the number of data points, better the degree of confidence (the accuracy) in the R-on-1 average value.

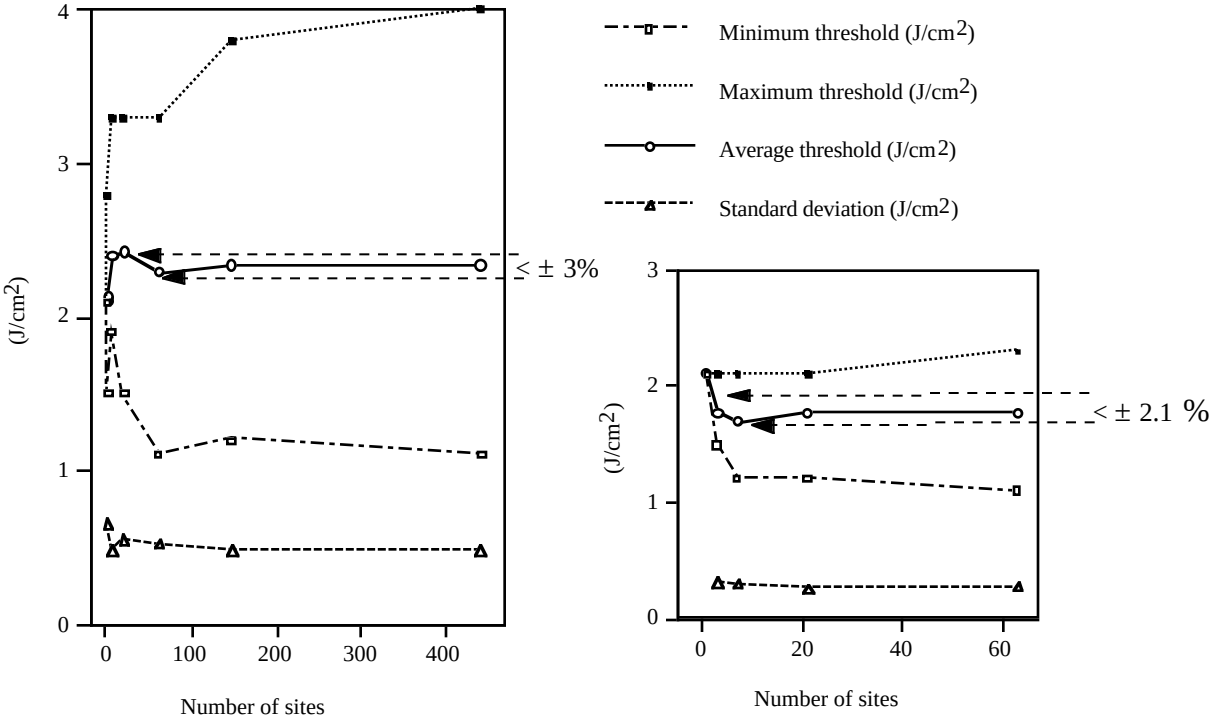

The average damage threshold is close to a constant :
2.29 J/cm^2 ≤ μ(s,n) ≤ 2.43 J/cm^2 for n=number of sites ≥ 7

Beam size = s

Figure 3a

The average damage threshold is close to a constant :
1.70 J/cm^2 ≤ μ(7s,n) ≤ 1.77 J/cm^2 for n=number of sites ≥ 3

Beam size = 7s

Figure 3b

For a given beam size, the R-on-1 average threshold quickly becomes constant
Figure 3

2.3 Threshold distribution

2.3.1 Experimental threshold distribution of small-area optics "s"

In Figure 4, the entire data of Figure 1 is sorted in 15 bins of 0.2 J/cm^2. On the same graph, the normal law for this set of data is also plotted (average threshold=μ=2.36 J/cm^2, standard deviation= σ=0.48 J/cm^2).

Though not perfect, the agreement between the experimental law and the theoretical normal law is rather close. Similarly, all the R-on-1 threshold distributions are not normal. Using a normal distribution has the advantage that the average and the standard deviation perfectly characterize this distribution. Moreover, it will allow to describe our method by avoiding heavy calculations. However, the described method works whatever the shape of the threshold distribution found.

The concept of the threshold distribution is powerful since even missing the site which presents the lowest damage threshold : the distribution allows a prediction of the behavior of the population with a high degree of confidence. In this case, the population is made by optics with a surface s=1mm^2 (s=area of the beam size). 50% of these optics will have a threshold equal to 2.35 J/cm^2= DT(s,50%) and 99.5% of these optics will have a damage threshold equal to 1.1 J/cm^2=DT(s,99.5%).

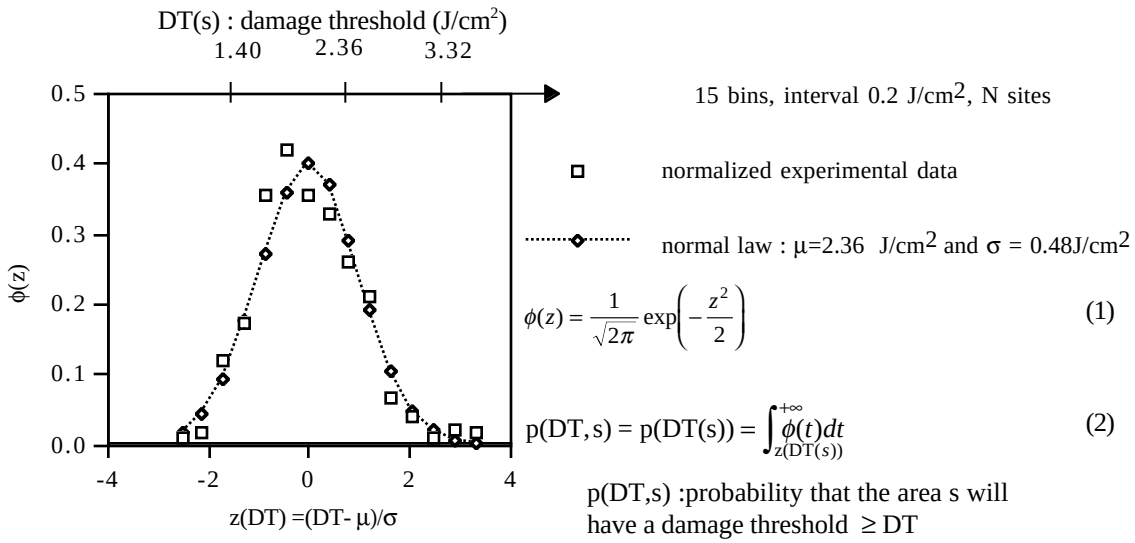

Experimental normalized data of Figure 1 and theoretical normal law ($\mu(s)=2.36$ J/cm^2, $\sigma(s)=0.48$ J/cm^2).
Figure 4

2.3.2 Threshold distribution for a population of large-area S

The ultimate goal is to determine the threshold of an optic with an area S, typically equal to 0.25 m^2, not to determine the threshold of an area s (=1mm^2) as done in Figure 4. If an optic of area S has a threshold DT, it means that the entire area S has to survive to a peak fluence equal or higher than DT. A surface S will have the probability $p(DT,S) = p(DT,s)^{S/s}$ to have a threshold DT (see Fig.5).

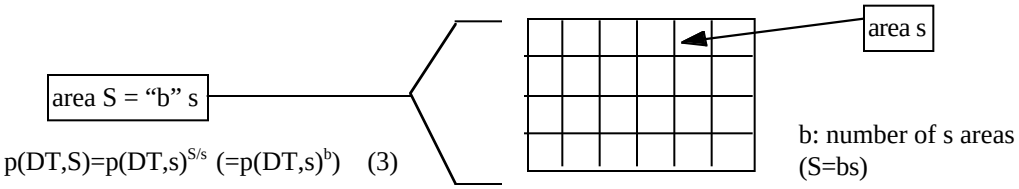

$p(DT,S)=p(DT,s)^{S/s}$ $(=p(DT,s)^{b})$ (3)

p(DT,S') : probability that the optic of area S'will have a threshold ≥DT

How calculate the threshold distribution for optics with a size S ?
Figure 5

To minimize the underestimation of p(DT,S), the 21s beam size distribution is taken into account. For this beam size, the standard deviation is minimum (Figs.2). It is assumed that with this beam size the threshold distribution also leads to a normal law. The experimental results supply $\mu(21s)=1.65$ J/cm^2 and $\sigma(21s)=0.23$ J/cm^2 for the 21s beam size distribution (Figs.2). So, Figure 7 is plotted using $p(DT,S)=p(DT,21s)^{S/21s}$ with $p(DT,21s) = \int_{z(DT(21s))=\frac{DT(21s)-\mu(21s)}{\sigma(21s)}}^{+\infty} \phi(t)dt$. It is easy to determine p(DT,21s) from μ and σ from a table[16] for z≥-4. For z=<-4, a method is shown in the appendix 7.1.

Figure 6 shows that there is a factor 2.2 (DT(s,99.5%)/DT(S,99.5%)= 1.1 Jcm^{-2}/ 0.5 Jcm^{-2}, in both cases the degree of confidence is 99.5 %) between the threshold of a small sample s and a large sample $S=25 .10^4$ s. Let us notice that the model shown may underestimate the threshold of a surface S (this point may be avoided by increasing the number of data taken on the witness sample).

The information in Figure 6, drawn from experimental data, is essential. Moreover, it outlines the difficulty and the danger to study the validation of a process using the damage threshold value of a single sample (large or small). The R-on-1 average on the other hand provides reliable information.

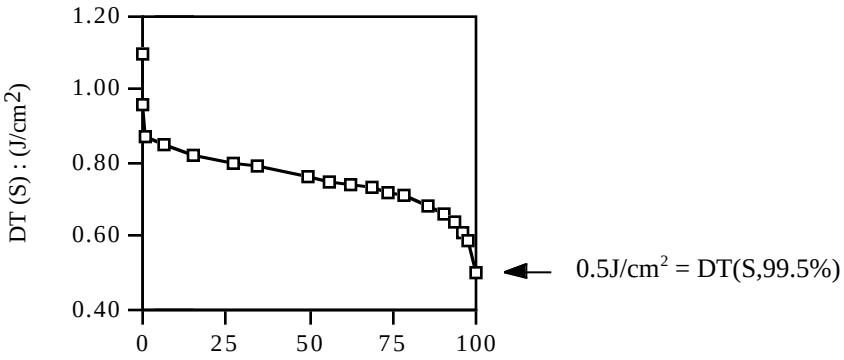

Threshold distribution for optics with a surface S using the experimental threshold distribution s.
This plot could be the typical threshold distribution of large optics (S) coming out the production.
Threshold distribution for large optics (S = 0.25 m^2)
Figure 6

2.3.4 Prediction of a large-area threshold with a computer

To predict a safe irradiation level with a high degree of confidence, the threshold distribution of LMJ or NIF large optics must be known. To reach this goal, the following method is proposed.

1-Determining the experimental distribution for the spot size s (Fig.5)

2-Proposing a fit for this experimental distribution (above all for the low values)

3-Computer simulating the threshold of a large optic (size S) using this experimental distribution (s)

3.a Number of trials equals to S/s

3.b Threshold of a surface S : the lowest value among the S/s values obtained (low pass filter)

4-Determining the threshold distribution of a large optic (size S) : do step 3 as many times as necessary to obtain this distribution

5-The final distribution (S) gives the desired answer (plot similar to Fig. 6 : threshold versus degree of confidence).

2.4 Conclusion

Two important new facts are shown. First, for a given beam size, the value of the R-on-1 average threshold and the standard deviation are quickly and accurately determined (few tests). Therefore, it is interesting to use these two parameters to compare different tests or samples, keeping in mind that it is not the threshold value of the final component.

Secondly, the concept of the threshold distribution seems very powerful to predict the threshold of a large-aperture component from the experimental threshold distribution obtained with a small spot size. A decrease of a factor of about 2 between the threshold of a small witness and 25.10^4 times larger seems likely as shown in this section. This factor is linked to the shape of the threshold distribution in particular the left "tail". In the future, to argue this method, many damage threshold maps on witnesses with different sizes using different spot sizes will have to be examined. Other parameters can be introduced for this model to calculate the optimum size and the number of optics that can deliver the desired energy. Price considerations may also be added in this model.

Obviously, this modeling only makes sense if the threshold distribution on small optic (s) and on large optic (S) are similar, otherwise the results will be probably worse for the large-area.

3. DAMAGE SIZE VERSUS FLUENCE

Four morphologies[4,5,6] have been reported at 1064 nm on NIF hafnia-silica multilayer polarizers and mirrors produced by e-beam: pits, flat bottom pits, scalds and delaminates. On the sample taken to illustrate our discussion (a polarizer without overcoat), the major damage morphology observed is the

delaminate. For NIF, it is interesting to correlate the size with fluence. After a brief description of the experimental procedure and the presentation of the data, the results are discussed.

3.1 Experimental procedure

A 1-on-1 test at 1064 µm, in "S" polarization, for a 10-ns pulse with a 56^0 angle of incidence is made. The beam is Gaussian, with a radius ω_0 at 1/e approximately equal to 425 µm. In the text, g refers to a Gaussian beam. The 52 tested sites are spaced by 2.5 mm from one another in both X and Y directions. A row consists of 4 sites. The peak fluence is decreased along the Y direction and the peak fluence is almost constant along the X direction.

3.2 Results

Figure 7 shows a typical delaminate. It is almost oval with an average ratio between the small and large axis close to 0.67 either an angle of 48 degrees (slightly inferior to the angle of incidence). The damage is not a perfect ellipse but "a sharp ellipse" with a shape close to the beam print.

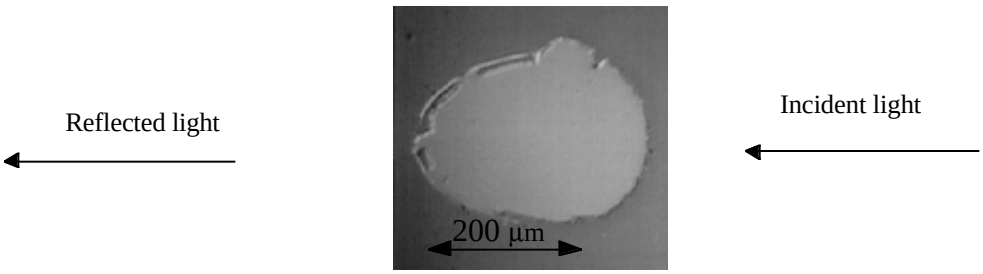

Nomarski micrograph of a typical delaminate on a polarizer tested at 10 ns, at $\theta=56^0$.
Figure 7

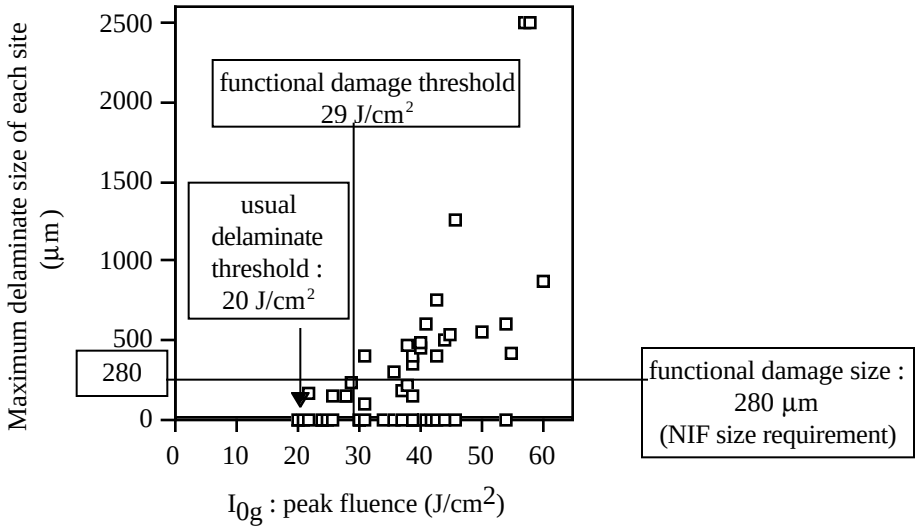

This polarizer is functional up to 29 J/cm^2 ; for this peak fluence, the damage size does not exceed 280 µm
52 tests : damage size versus peak fluence
Figure 8

In Figure 8, all the results are gathered. In a few cases, where many delaminates were found on the same site, their damage sizes were added. This method leads to an overestimation of the damaged area. One of the NIF requirements is that the damage size[17] be less than 280 µm. Figure 8 shows that the witness polarizers can sustain a peak fluence of 29 J/cm^2 without loss of functionality. The usual delaminate

threshold appears to be near 20 J/cm^2 (more data is needed to confirm this value). Let us note that the results are likely less reliable when the damage size is close (or larger) to the beam size.

Figure 8 shows significant scatter in damage sizes for a given fluence. For further analysis, the size data is grouped into seven fluence bins and averaged (Fig. 9). Both data sets can be fitted to a power law. Interpolation or extrapolation become possible and different samples can be compared. If the functional damage size requirement is changed, this data can be used to determine the new fluence limit. The raw data (Fig.8) and Figure 9 give very similar threshold values : 29 J/cm^2 and 28 J/cm^2, respectively, for a functional damage size of 280 µm.

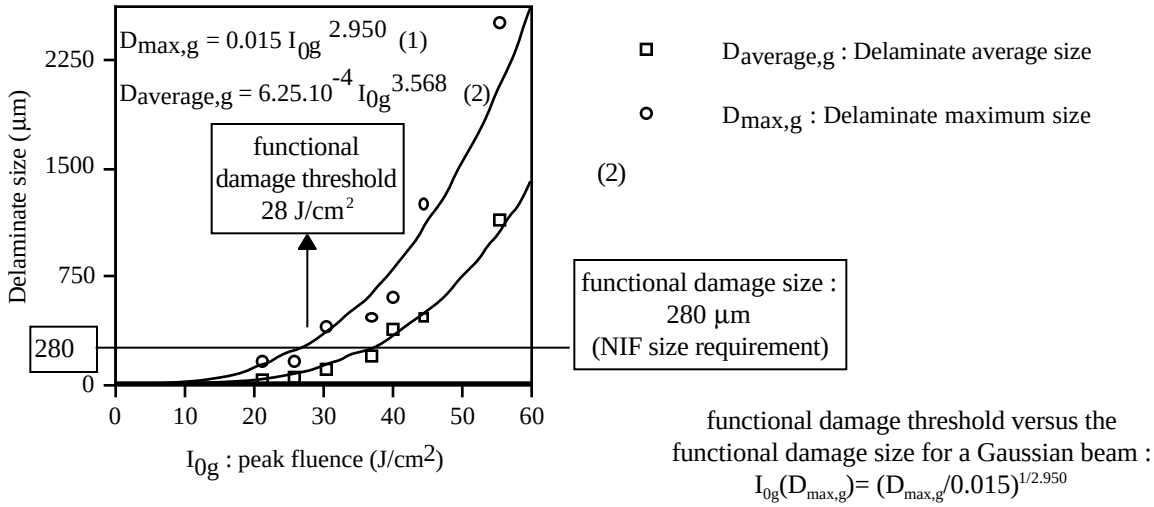

functional damage threshold versus the functional damage size for a Gaussian beam : $I_{0g}(D_{max,g}) = (D_{max,g}/0.015)^{1/2.950}$

Delaminate size versus peak fluence obtained with a carefully chosen average
Figure 9

3.3 Application of these results to determine the fractional damaged area

The percentage of obscuration (c) of the total area due to damage may be an another requirement for NIF. Furthermore, the beam used for NIF is not a Gaussian beam but a top-hat beam. Therefore, a condition for NIF is that :

$$\frac{\text{Damaged area}}{\text{Irradiated area}} = c \le c_{limit} \ . \qquad (4)$$

Since the damage has a symmetry similar to that of the beam print (see Fig. 9), the equation (4) becomes, at a beam incidence angle θ :

$$\frac{\text{Damage size}(\theta)}{\text{Characteristic irradiation size}(\theta)} = \sqrt{c} \le \sqrt{c_{limit}} \ . \qquad (5)$$

3.3.1 For a Gaussian beam

Let us see how the data in Figure 9 may be used to address this issue. The power law fit is :

$$D_{average,g}(I_{0g}) = D_{average,g}(I_{0g}, \omega_0) = D_{0g} I_{0g}^{\ \alpha} \ , \qquad (6)$$

where g indicates a Gaussian beam, I_{0g} is the peak fluence and ω_0 the radius at 1/e.

Combining (5) and (6) :

$$\sqrt{c} = \frac{D_{0g} I_{0g}^{\alpha}}{\frac{2\omega_0}{\cos(\theta)}} \ , \qquad (7)$$

therefore, $I_{0g}(c)\ (J/cm^2) = \left(\frac{2\sqrt{c}\omega_0(\mu m)}{\cos(\theta) D_{0g}(\mu m)} \right)^{\frac{1}{\alpha}}$ (8) with $I_{0g\ threshold} = I_{0g}(c_{limit})$. (9)

3.3.2 For a top-hat beam : Determination of $I_{0h}(c)$ by deconvolution

The goal is to obtain an equation similar to (6) and to (8) for a top-hat beam. With the empirical law (6), found for a gaussian beam, and assuming that the damage size is linked to the local fluence but also to the percentage of the fluence seen by the sample, it is obtained :

$$D_{0g} I_{0g}^{\alpha} = \int_{I(r=0)/I_{0g}}^{I(r=+\infty)/I_{0g}} D_{average,h}(I(r)) \; . \; d(I(r)/I_{0g}) \qquad (10)$$

$$\text{with} \quad I(r) = I_{0g} \; \exp\left(-\frac{r^2}{\omega_0^2}\right). \qquad (11)$$

Assuming that $D_{average,h}(I_{0h}) = D_{0h} \, I_{0h}^{\beta}$; (12)

(10), (11) and (12) lead to : $D_{average,h}(I_{0h}) = D_{0g}(1+\alpha) I_{0h}^{\alpha}$. (13)

Combining (5) and (13), it is obtained : $I_{0h}(c) = \frac{1}{(1+\alpha)^{1/\alpha}} \; I_{0g}(c)$ (14)

In this particular case, with $\alpha = 3.568$, $I_{0h}(c) \approx 0.65 \, I_{0g}(c)$ (15)

A method by underestimation and by overestimation is shown in Appendix 7.3. It leads to a similar result than (15). The link proposed between the threshold obtained with a Gaussian and a top-hat beam is only based on energy considerations. The knowledge of the delaminate occurrence could confirm if this assumption is valid or not.

3.3.3 Discussion

Using (8) and (14), the delaminate threshold can be evaluated for different values of c (the percentage of damaged area) as reported in Figure 10. If c_{limit} is defined, Figure 10 leads directly to a new threshold value. Since a value of c_{limit} is not defined, Figure 10 can be used to determine what fractional area is damaged for the functional damage threshold determined previously. In this particular case, the fractional damage area will be about 0.4% (Fig.10). A top-hat beam of 18.2 J/cm^2 will lead to the same fractional damage area (Fig.10).

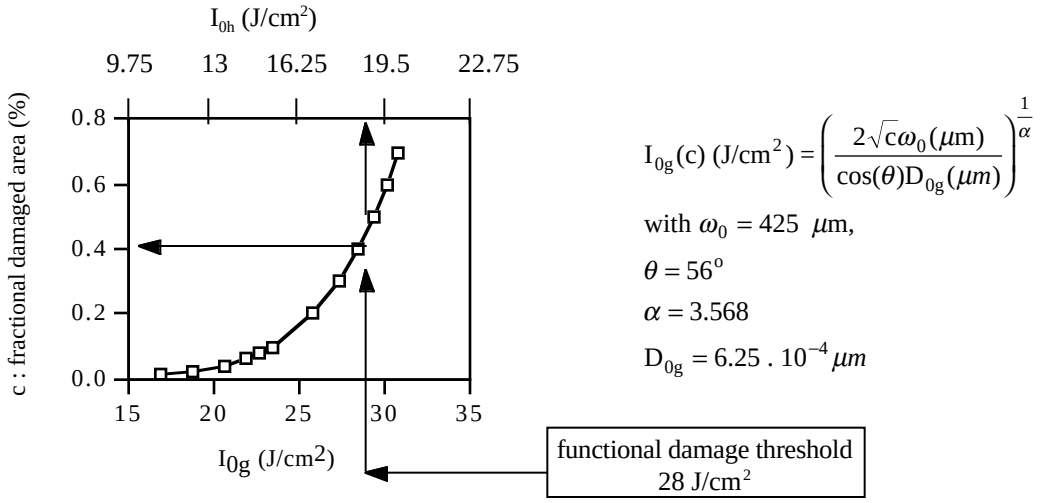

Delaminate threshold versus fractional damaged total area
Figure 10

3.4 Summary and conclusion

Following the definitions used and depending on the requirements, three damage threshold values can be given for the delaminates of this polarizer :

- the occurrence of the first delaminates : 20 J/cm^2,

- the condition of maximum 280 µm damage size : 28 J/cm^2 -29 J/cm^2,
- the fractional damaged area for an obscuration smaller than c_{limit} .

Empirical power laws dependence of the average delaminate size and of the maximum delaminate size on peak fluence were found. According to the criteria chosen, the interpolation of these laws can easily provide a functional damage threshold. The previous laws can also be used to establish the dependence of fractional damaged area on peak fluence.

This method to characterize the damage threshold brings more information than the usual method to obtain the threshold. These measurements better show the average behavior of a large-area optics. But they cannot claim to predict the threshold value of a large component. In this study, although the effect of the spot size was taken into account, the effect of a large beam is still undetermined.

4. CONCLUSION

The first part of this paper showed that the concept of the threshold distribution is very convenient to study the threshold in a reliable manner. This method can be used in research as well in production. With the average R-on-1 threshold, the improvement of the coating can be determined with a high degree of accuracy. The thought experiments from experimental data are very convenient to illustrate this point. With the threshold distribution itself, the percentage of the optics which will sustain a given fluence can be predicted. For optics which are not affected by conditioning (as most substrates, most ion beam sputtered coatings, or if the conditioning is a part of the process), the use of R-on-1 distribution seems to be a good way to characterize the damage threshold of the components. The key point of this technique is that all sites yield a threshold value. It is the reason why it becomes possible to obtain a threshold distribution. The threshold distribution is difficult to obtain with usual tests. Therefore, the real surface of the final component can be taken into account to evaluate its threshold with a high degree of confidence. The example chosen to illustrate this study shows that a decrease by a factor about 2 is likely between the threshold for a final component 25.10^4 larger than the spot size used in the test. Obviously, the exact factor depends on the shape of the distribution, in particular the “left” tail of the distribution.

The second part of this paper showed the correlation between delaminate size and peak fluence. An empirical power law dependence is found for both average and maximum delaminate size. As the experimental results are often spread, it becomes easy with this method to determine the value of the functional damage threshold according to a maximum damage size. The average damage size and the fractional damaged area as a function of the peak fluence only provide the mean behavior of a large optic (which can be far off of the extreme value which fixes the threshold of a large component). A method to use these data (obtained from a Gaussian beam) for a top-hat beam is proposed. To guarantee the validity of this last model, a knowledge of the delaminate occurrence has to be determined in order to test the assumptions based on energy considerations.

Both proposed techniques have the advantage of being independent of wavelength, pulse duration and optical component type. Moreover, they take into account the final size of the components.

5. ACKNOWLEDGMENT

This work performed under the auspices of the U. S. Department of Energy by Lawrence Livermore National Laboratory under Contract No. W-7405-ENG-48, under the auspices of the Laser MegaJoules Project (CEA/DAM/DLP), and the French Ministry of Defense (Group IV). Many thanks are expressed to Lynn Sheehan and Pierre Kumurdjian for their valuable comments.

6. REFERENCES

1. J. Hue, J. Dijon, P. Lyan, “The CMO YAG damage test facility”, Laser Damage In Optical Materials 1995 , SPIE 2714, pp. 102-113.

2. B.E. Yoldas, D.P. Partlow, “A wide spectrum antireflective coating for silica optics and its damage resistance at 350 nm”, Laser Damage In Optical Materials 1983, NBS Special Publication 688, pp. 407-416.

3. S.R. Foltyn, L.J. Jolin, “Catastrophic versus microscopic damage : applicability of laboratory measurements to real system”, Laser Damage In Optical Materials 1983, NBS Special Publication 688, pp. 493-501.

4. L. Sheehan, M. Kozlowski, C. Stolz, F. Génin, M. Runkel, S. Schwartz, J. Hue, "Large-area damage testing of optics", *Int. Symp. On Optical Systems Design And Production*, Glasgow, U.K., May 1996.
5. F.Y. Génin, C.J. Stolz, M.R. Kozlowski, "Growth of damage during repetitive illumination at 1064 nm in hafnia-silica mirrors and polarizers", to be published in these proceedings
6. F.Y. Génin, C.J. Stolz, "Morphologies of laser-induced damage in hafnia-silica multilayer mirror and polarizer coatings", *3rd Int. Workshop On Laser Beam And Optics Characterization*, Québec, Canada, Aug. 1996.
7. S.R. Foltyn, "Spotsize effects in laser damage testing", Laser Damage In Optical Materials 1982, NBS Special Publication 669, pp. 368-379.
8. S.C. Seitel, J.O. Porteus, "Toward improved accuracy in limited-scale pulsed laser damage testing via the onset method", Laser Damage In Optical Materials 1983, NBS Special Publication 688, pp. 502-512.
9. J.O. Porteus, S.C. Seitel, "Absolute onset of optical surface damage using distributed defect ensembles", Applied optics, Vol. **23**, N^0 21, 1 November 1984, pp. 3796-3805.
10. Draft International Standard ISO/DIS 11254, "Optics and optical instruments-Laser and laser related equipment. Test methods for laser induced damage threshold of optical surfaces.
11. J.R. Arenberg, "A revised damage frequency method for the determination of laser damage threshold", Laser Damage In Optical Materials 1993, SPIE 2114, pp. 521-526
12. J.R. Arenberg, " Determination of minimal test sample size for high accuracy laser damage testing", Laser Damage In Optical Materials 1994, SPIE 2428, pp. 486-488
13. W.H. Lowdermilk, D. Milam, "Laser-induced surface and coating damage", IEEE Journal of Quantum Electronics, Vol. QE-**17**, N^{0}19, September 1981, pp. 1888-1903.
14. L. Sheehan, M. Kozlowski, F. Rainer, M. Staggs, "Large-area conditioning of optics for high-power laser systems", Laser Damage In Optical Materials 1993,SPIE 2114, pp. 82-86..
15. J. Hue, P. Garrec, J. Dijon, P. Lyan, "R-on-1 automatic mapping : a new tool for laser damage testing", Laser Damage In Optical Materials 1995, SPIE 2714, pp. 90-101.
16. E.B. Mode ,*"Elements probability and statistics"*, Prentice-Hall, Inc, 1966.
17. J.T. Hunt, K.R. Manes, P.A. Renard, Applied Optics, Vol. **32**, N^0 30, 1993, p 5793.
18. M. Abramowitz, I.A. Stegun, *"Handbook of mathematical functions"*, Applied Mathematics series 55, NBS, Washington, 1964
19. J. Dijon, P. Garrec, N. Kaiser, "Influence of substrate cleaning on LIDT of 355 nm HR coatings", to be published in these proceedings.

7. APPENDIX

7.1 Area under a normal curve

As usually after z=-4 the areas under a normal curve are not available in the tables, an approximation is given from the formula [18] :

$$\frac{1}{z+\sqrt{z^2+2}} < e^{z^2}\int_z^{+\infty} e^{-t^2}dt \le \frac{1}{z+\sqrt{z^2+\frac{4}{\pi}}} \qquad (16) \quad \text{for } z \ge 0 \ .$$

(16) leads to :

$$1-\frac{1}{\sqrt{\pi}}\frac{1}{e^{\frac{z^2}{2}}\left(-\frac{z}{\sqrt{2}}+\sqrt{\frac{z^2}{2}+\frac{4}{\pi}}\right)} \le p(-z) < 1-\frac{1}{\sqrt{\pi}}\frac{1}{e^{\frac{z^2}{2}}\left(-\frac{z}{\sqrt{2}}+\sqrt{\frac{z^2}{2}+2}\right)} \qquad (17)$$

with $p(-z) = \int_{-\infty}^{-z}\phi(t)dt = 1 - \int_{-z}^{+\infty}\phi(t)dt$ for $z \ge 0$ (18) with $z = z(DT) = \frac{DT - \mu}{\sigma}$

-z	1-p(-z)
4.1	2.080E-5
4.2	1.343E-5
4.3	8.695E-6
4.4	5.448E-6
4.5	3.419E-6
4.6	2.125E-6
5	2.882E-7

table 1

So the formula (17) is used to calculate the value in the table 1 and to plot Figure 6.

7.2 Threshold of a "standard" large sample S

Let us examine a simple model which will not provide a threshold distribution but only the threshold of a "standard" sample S (e.g. DT(S,50%)). Let us build up by the thought an optic S from the distribution of 21s (μ(21s)=1.65 J/cm^2 and σ(21s)=0.23 J/cm^2). As seen previously, S/21s samples are needed to recreate a surface S from optic with a size s. Let us imagine the "standard" sample S represents faithfully the 21s threshold distribution. In this case the lower limit,

$-z(DT(S,50\%)) = -(DT(S,50\%) - \mu(21s))/\sigma(21s)$ which satisfies $\int_{-z(DT)}^{+z(DT)} \phi(t)dt = 1 - 21s/S$, (18)

will give the threshold. In this case, it leads to $-z(DT(S,50\%)) = -4$, hence to $DT(S,50\%) = 0.73$ J/cm^2. This value has to be close from the threshold reached by about 50% of large optics ("standard" sample). This result is consistent with the Figure 6 which gives $DT(S,68\%) = 0.73$ J/cm^2.

7.3 Determination of $I_{0h}(c)$ by an underestimation and by an overestimation

It is assumed that the wings of the Gaussian beam (the fluence for $r > \omega_0$) have not any effect on the formula (6). If the Gaussian beam (I_{0g},ω_0) is replaced by a top-hat beam ($I_{0h} = I_{0g},\omega_0$) (h refers to a top-hat beam) with the same energy and with the same radius, $D_{average,g}(I_{0g},\omega_0)$ will be an underestimate for $D_{average,h}$ (I_{0h},ω_0) (top-hat beam profile **(2)** Fig.11a). If the Gaussian beam (I_{0g},ω_0) is replaced by a top-hat beam ($I_{0h}' = I_{0g}/e,\omega_0$), $D_{average,g}(I_{0g},\omega_0)$ will be an overestimation for $D_{average,h}(I_{0h}',\omega_0)$ (top-hat beam profile **(3)** Fig.11a). Therefore, the better way is to replace the Gaussian beam (I_{0g},ω_0) by a top-hat beam (I_{0h}'',ω_0) where I_{0h}'' is determined so that the Gaussian beam (profile **(4)** Fig.11b : Gaussian beam without wings) and the top-hat beam between r=0 and $r=\omega_0$ have the same energy (profile **(5)** Fig.11b). It leads to $I_{0h}'' = (1-1/e)\, I_0 = 0.63\, I_{0g} = 0.63\, I_{0h}$

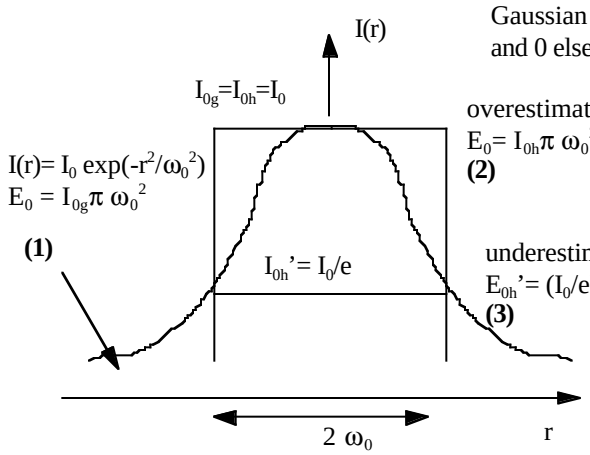

Figure 11a

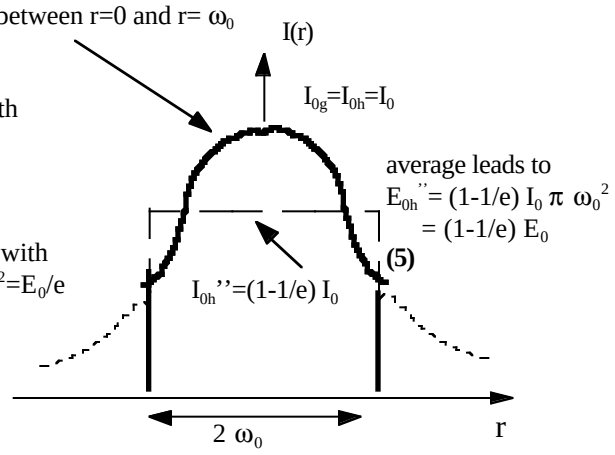

Figure 11b

The Gaussian beam **(1)** and the top-hat beam **(2)** have the same energy E_0.
The top-hat beam **(3)** have the energy E_0 /e. **(4)** and **(5)** have the same energy (1-1/e) E_0

Figures 11

All this discussion is summarized by :

$$D_h\left(I_{0h}' = \frac{I_{0g}}{e}\right) < D_g(I_{0g}) = D_{0g}I_{0g}^{\alpha} \approx D_h(I_{0h}'' = (1-1/e)I_{0g} = 0.63I_{0g}) < D_h\,(I_{0h} = I_{0g}), \quad (19)$$

$$\text{hence } D_{average,g}(I_{0g}) = D_{0g}I_{0g}^{\alpha} \approx D_{average,h}(0.63I_{0g}). \quad (20)$$

$$\text{therefore } I_{0h}(c) = 0.63\, I_{0g}(c), \quad (21)$$

$$\text{and } D_h(I_{0h}) = (D_{0g}/0.63^{\alpha})\, I_{0h}^{\alpha}. \quad (22)$$

The difference, between the results (14) and (21), concerns the coefficient which is always constant in the first case and in the other case varies between 1/e and 1 for α between 0 and infinite. Let us notice that in both cases the asymptotic values of α lead to non physical cases for the damage size because this type of fit has no physical sense. Whatever the results used (e.g. (14) and (21)), the fluences are almost the same : $2 < \alpha < 5$ ==> $0.58 < 1/(1+\alpha)^{1/\alpha} < 0.69$ in comparison to 0.63=(1-1/e).

Technical Information Department • **Lawrence Livermore National Laboratory**
University of California • Livermore, California 94551